



SPIN PHYSICS AT NICA



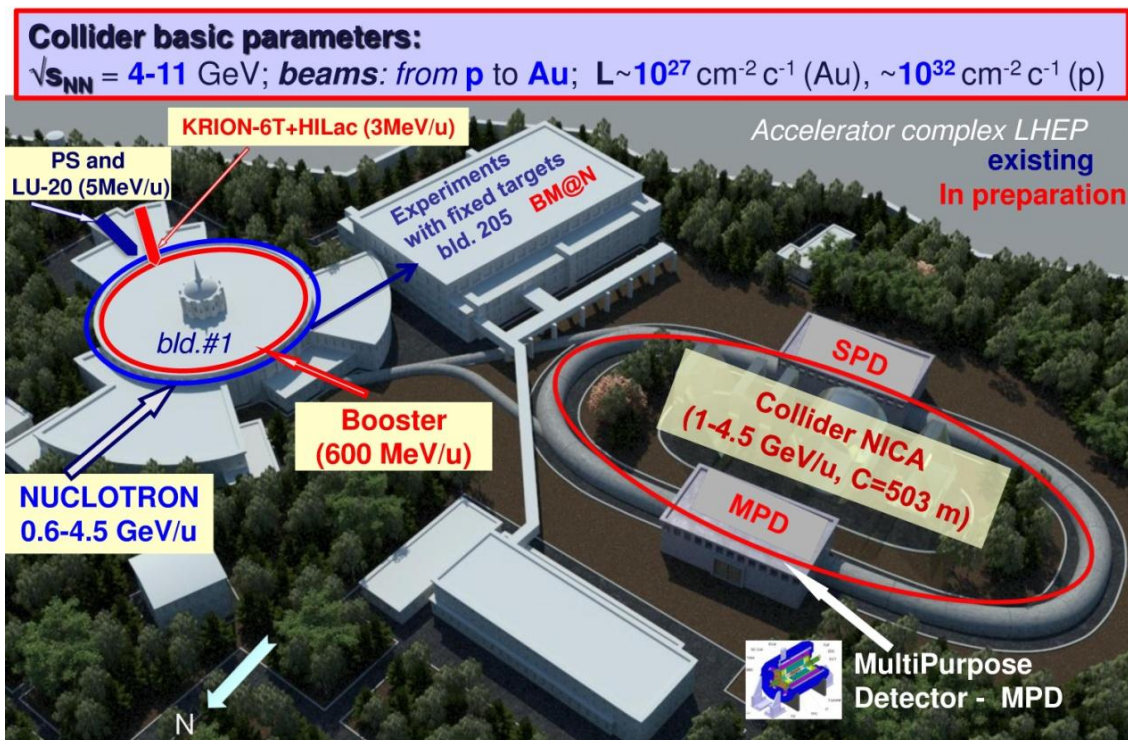
A.P. Nagaytsev, JINR, Dubna

on materials of LoI:

“Spin Physics Experiments at NICA-SPD with polarized proton and deuteron beams”,

I.A. Savin, A.V. Efremov, D.V. Peshekhonov, A.D. Kovalenko, O.V. Teryaev, O. Yu. Shevchenko,
 A.P. Nagaytsev, A.V. Guskov, V.V. Kukhtin, N.D. Topilin (Dubna, JINR). Aug 18, 2014. , arXiv:1408.3959

1. Introduction.
2. Physics motivations.
3. SPD detector.
4. Proposed measurements.
5. Future DY experiments.
6. Outlook.

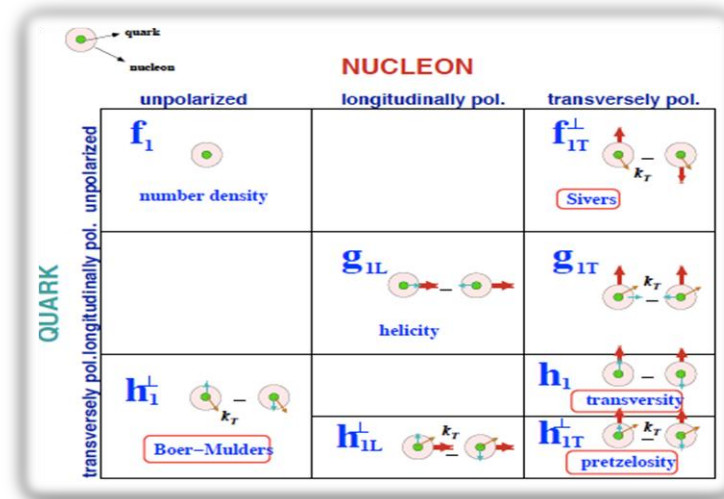


1. Introduction.

Main parts of this Letter of Intent (LoI) are related to the studies of the nucleon structure.

Now the quark-parton structure of nucleons and respectively the quark-parton model of nucleons are becoming more and more complicated. In Quantum Chromo Dynamics (QCD), PDFs depend not only on x , but also on Q^2 , four-momentum transfer (see below). Partons can have an internal momentum, k , with possible transverse component, k_T . A number of PDFs depends on the order of the QCD approximations. Measurements of the collinear (integrated over k_T) and Transverse Momentum Dependent (TMD) PDFs, the most of which are not well measured or not discovered yet, are proposed in this LoI (e-Print:arXiv:1408.3959).

	U	L	T	
U	f_1 Number Density		h_1^\perp Boer-Mulders	T-odd
L		g_1 Helicity	h_{1L}^\perp Worm-gear-L	
T	f_{1T}^\perp Sivers	g_{1T}^\perp Worm-gear-T	h_1 Transversity h_{1T}^\perp Pretzelosity	chiral-odd





2. Physics motivations.

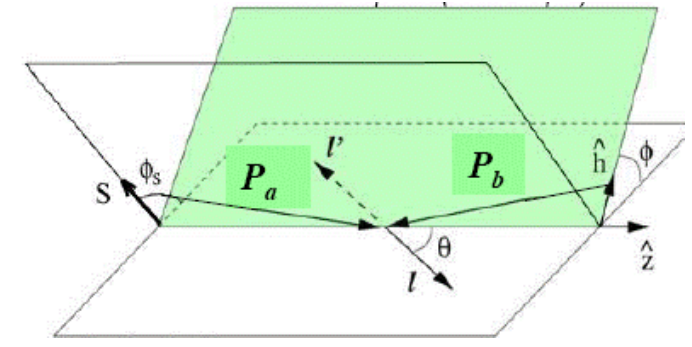
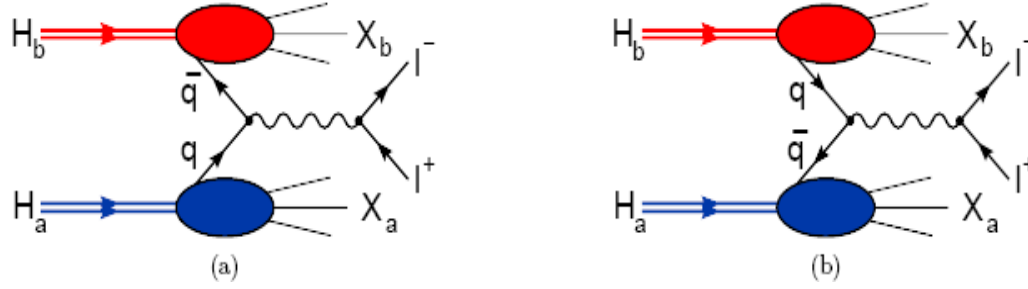


The main physical tasks proposed for spin program at NICA are as follows:

- ▶ Nucleon spin structure studies using the Drell-Yan reactions.
- ▶ Direct photons.
- ▶ New nucleon PDFs and J/Ψ production.
- ▶ Spin-dependent effects in elastic pp, pd and dd scattering.
- ▶ Spin effects in one and two hadron production processes.
- ▶ Spin-dependent high- p_T reactions.
- ▶ Spin-dependent reactions in heavy ion collisions.

2. Physics motivations.

Nucleon spin structure studies using the Drell-Yan reactions.
The PDFs studies via asymmetry of the Drell-Yan pairs.



$$\frac{d\sigma}{dx_a dx_b d^2q_T d\Omega} = \frac{\alpha^2}{4Q^2} \times$$

$$\left\{ \left((1 + \cos^2 \theta) F_{UU}^1 + \sin^2 \theta \cos 2\phi F_{UU}^{\cos 2\phi} \right) + S_{aL} \sin^2 \theta \sin 2\phi F_{LU}^{\sin 2\phi} + S_{bL} \sin^2 \theta \sin 2\phi F_{UL}^{\sin 2\phi} \right.$$

$$\left. + \left| \vec{S}_{aT} \right| \left[\frac{\sin(\phi - \phi_{S_a})}{\text{Lepton plane}} (1 + \cos^2 \theta) F_{TU}^{\sin(\phi - \phi_{S_a})} + \sin^2 \theta \left(\sin(3\phi - \phi_{S_a}) F_{TU}^{\sin(3\phi - \phi_{S_a})} + \sin(\phi + \phi_{S_a}) F_{TU}^{\sin(\phi + \phi_{S_a})} \right) \right] \right.$$

$$\left. + \left| \vec{S}_{bT} \right| \left[\sin(\phi - \phi_{S_b}) (1 + \cos^2 \theta) F_{UT}^{\sin(\phi - \phi_{S_b})} + \sin^2 \theta \left(\sin(3\phi - \phi_{S_b}) F_{UT}^{\sin(3\phi - \phi_{S_b})} + \sin(\phi + \phi_{S_b}) F_{UT}^{\sin(\phi + \phi_{S_b})} \right) \right] \right.$$

$$\left. + S_{aL} S_{bL} \left[(1 + \cos^2 \theta) F_{LL}^1 + \sin^2 \theta \cos 2\phi F_{LL}^{\cos 2\phi} \right] \right. \quad (2.1.2)$$

$$\left. + S_{aL} \left| \vec{S}_{bT} \right| \left[\cos(\phi - \phi_{S_b}) (1 + \cos^2 \theta) F_{LT}^{\cos(\phi - \phi_{S_b})} + \sin^2 \theta \left(\cos(3\phi - \phi_{S_b}) F_{LT}^{\cos(3\phi - \phi_{S_b})} + \cos(\phi + \phi_{S_b}) F_{LT}^{\cos(\phi + \phi_{S_b})} \right) \right] \right.$$

$$\left. + \left| \vec{S}_{aT} \right| S_{bL} \left[\cos(\phi - \phi_{S_a}) (1 + \cos^2 \theta) F_{TL}^{\cos(\phi - \phi_{S_a})} + \sin^2 \theta \left(\cos(3\phi - \phi_{S_a}) F_{TL}^{\cos(3\phi - \phi_{S_a})} + \cos(\phi + \phi_{S_a}) F_{TL}^{\cos(\phi + \phi_{S_a})} \right) \right] \right.$$

$$\left. + \left| \vec{S}_{aT} \right| \left| \vec{S}_{bT} \right| \left[(1 + \cos^2 \theta) \left(\cos(2\phi - \phi_{S_a} - \phi_{S_b}) F_{TT}^{\cos(2\phi - \phi_{S_a} - \phi_{S_b})} + \cos(\phi_{S_b} - \phi_{S_a}) F_{TT}^{\cos(\phi_{S_b} - \phi_{S_a})} \right) \right] \right.$$

$$\left. + \left| \vec{S}_{aT} \right| \left| \vec{S}_{bT} \right| \left[\sin^2 \theta \left(\cos(\phi_{S_a} + \phi_{S_b}) F_{TT}^{\cos(\phi_{S_a} + \phi_{S_b})} + \cos(4\phi - \phi_{S_a} - \phi_{S_b}) F_{TT}^{\cos(4\phi - \phi_{S_a} - \phi_{S_b})} \right) \right] \right.$$

$$\left. + \left| \vec{S}_{aT} \right| \left| \vec{S}_{bT} \right| \left[\sin^2 \theta \left(\cos(2\phi - \phi_{S_a} + \phi_{S_b}) F_{TT}^{\cos(2\phi - \phi_{S_a} + \phi_{S_b})} + \cos(2\phi + \phi_{S_a} - \phi_{S_b}) F_{TT}^{\cos(2\phi + \phi_{S_a} - \phi_{S_b})} \right) \right] \right\}$$

The cross section cannot be measured directly because there is no single beam containing particles with the U, L and T polarization. To measure SFs entering this equation one can use the following procedure: first, to integrate cross section over the azimuthal angle ϕ_s , second, following the SIDIS practice, to measure azimuthal asymmetries of the DY pair's production cross sections. The integration over the azimuthal angle ϕ gives:

$$\sigma_{\text{int}} \equiv \frac{d\sigma}{dx_a dx_b d^2q_T d \cos \theta} = \frac{\pi \alpha^2}{2q^2} \times (1 + \cos^2 \theta) \left[F_{UU}^1 + S_{aL} S_{bL} F_{LL}^1 \right.$$

$$\left. + \left| \vec{S}_{aT} \right| \left| \vec{S}_{bT} \right| \left(\cos(\phi_{S_b} - \phi_{S_a}) F_{TT}^{\cos(\phi_{S_b} - \phi_{S_a})} + D \cos(\phi_{S_a} + \phi_{S_b}) F_{TT}^{\cos(\phi_{S_a} + \phi_{S_b})} \right) \right]$$

where F_{jk}^i are the Structure Functions (SFs) connected to the corresponding PDFs. The SFs depend on four variables $P_a \cdot q$, $P_b \cdot q$, \mathbf{q}_T and q^2 or on \mathbf{q}_T , q^2 and the Bjorken variables of colliding hadrons, x_a , x_b ,

$$x_a = \frac{q^2}{2P_a \cdot q} = \sqrt{\frac{q^2}{s}} e^y, \quad x_b = \frac{q^2}{2P_b \cdot q} = \sqrt{\frac{q^2}{s}} e^{-y}, \quad y \text{ is the CM rapidity and}$$

2. Physics motivations.

Nucleon spin structure studies using the DY reactions.
The PDFs studies via asymmetry of the Drell-Yan pair.

$$A_{UU} \equiv \frac{\sigma^{00}}{\sigma_{\text{int}}^{00}} = \frac{1}{2\pi} (1 + D \cos 2\phi A_{UU}^{\cos 2\phi})$$

$$A_{LU} \equiv \frac{\sigma^{\rightarrow 0} - \sigma^{\leftarrow 0}}{\sigma_{\text{int}}^{\rightarrow 0} + \sigma_{\text{int}}^{\leftarrow 0}} = \frac{|S_{aL}|}{2\pi} D \sin 2\phi A_{LU}^{\sin 2\phi}$$

$$A_{UL} \equiv \frac{\sigma^{0\rightarrow} - \sigma^{0\leftarrow}}{\sigma_{\text{int}}^{0\rightarrow} + \sigma_{\text{int}}^{0\leftarrow}} = \frac{|S_{bL}|}{2\pi} D \sin 2\phi A_{UL}^{\sin 2\phi}$$

$$A_{TU} \equiv \frac{\sigma^{\uparrow 0} - \sigma^{\downarrow 0}}{\sigma_{\text{int}}^{\uparrow 0} + \sigma_{\text{int}}^{\downarrow 0}} = \frac{|\vec{S}_{aT}|}{2\pi} \left[A_{TU}^{\sin(\phi - \phi_{S_a})} \sin(\phi - \phi_{S_a}) + D \left(A_{TU}^{\sin(3\phi - \phi_{S_a})} \sin(3\phi - \phi_{S_a}) + A_{TU}^{\sin(\phi + \phi_{S_a})} \sin(\phi + \phi_{S_a}) \right) \right]$$

$$A_{UT} \equiv \frac{\sigma^{0\uparrow} - \sigma^{0\downarrow}}{\sigma_{\text{int}}^{0\uparrow} + \sigma_{\text{int}}^{0\downarrow}} = \frac{|\vec{S}_{bT}|}{2\pi} \left[A_{UT}^{\sin(\phi - \phi_{S_b})} \sin(\phi - \phi_{S_b}) + D \left(A_{UT}^{\sin(3\phi - \phi_{S_b})} \sin(3\phi - \phi_{S_b}) + A_{UT}^{\sin(\phi + \phi_{S_b})} \sin(\phi + \phi_{S_b}) \right) \right]$$

$$A_{LL} \equiv \frac{\sigma^{\rightarrow\rightarrow} + \sigma^{\leftarrow\leftarrow} - \sigma^{\leftarrow\rightarrow} - \sigma^{\rightarrow\leftarrow}}{\sigma_{\text{int}}^{\rightarrow\rightarrow} + \sigma_{\text{int}}^{\leftarrow\leftarrow} + \sigma_{\text{int}}^{\leftarrow\rightarrow} + \sigma_{\text{int}}^{\rightarrow\leftarrow}} = \frac{|S_{aL} S_{bL}|}{2\pi} \left(A_{LL}^1 + D A_{LL}^{\cos 2\phi} \cos 2\phi \right)$$

$$A_{\pi L} \equiv \frac{\sigma^{\uparrow\rightarrow} + \sigma^{\downarrow\leftarrow} - \sigma^{\downarrow\rightarrow} - \sigma^{\uparrow\leftarrow}}{\sigma_{\text{int}}^{\uparrow\rightarrow} + \sigma_{\text{int}}^{\downarrow\leftarrow} + \sigma_{\text{int}}^{\downarrow\rightarrow} + \sigma_{\text{int}}^{\uparrow\leftarrow}} = \frac{|\vec{S}_{aT}| |S_{bL}|}{2\pi} \left[A_{\pi L}^{\cos(\phi - \phi_{S_a})} \cos(\phi - \phi_{S_a}) + D \left(A_{\pi L}^{\cos(3\phi - \phi_{S_a})} \cos(3\phi - \phi_{S_a}) + A_{\pi L}^{\cos(\phi + \phi_{S_a})} \cos(\phi + \phi_{S_a}) \right) \right]$$

$$A_{LT} \equiv \frac{\sigma^{\rightarrow\uparrow} + \sigma^{\leftarrow\downarrow} - \sigma^{\leftarrow\uparrow} - \sigma^{\rightarrow\downarrow}}{\sigma_{\text{int}}^{\rightarrow\uparrow} + \sigma_{\text{int}}^{\leftarrow\downarrow} + \sigma_{\text{int}}^{\leftarrow\uparrow} + \sigma_{\text{int}}^{\rightarrow\downarrow}} = \frac{S_{aL} |\vec{S}_{bT}|}{2\pi} \left[A_{LT}^{\cos(\phi - \phi_{S_b})} \cos(\phi - \phi_{S_b}) + D \left(A_{LT}^{\cos(3\phi - \phi_{S_b})} \cos(3\phi - \phi_{S_b}) + A_{LT}^{\cos(\phi + \phi_{S_b})} \cos(\phi + \phi_{S_b}) \right) \right]$$

$$A_{TT} \equiv \frac{\sigma^{\uparrow\uparrow} + \sigma^{\downarrow\downarrow} - \sigma^{\uparrow\downarrow} - \sigma^{\downarrow\uparrow}}{\sigma_{\text{int}}^{\uparrow\uparrow} + \sigma_{\text{int}}^{\downarrow\downarrow} + \sigma_{\text{int}}^{\uparrow\downarrow} + \sigma_{\text{int}}^{\downarrow\uparrow}} = \frac{|\vec{S}_{aT}| |\vec{S}_{bT}|}{2\pi} \left[A_{TT}^{\cos(2\phi - \phi_{S_a} - \phi_{S_b})} \cos(2\phi - \phi_{S_a} - \phi_{S_b}) + A_{TT}^{\cos(\phi_{S_b} - \phi_{S_a})} \cos(\phi_{S_b} - \phi_{S_a}) \right]$$

$$+ D \left(A_{TT}^{\cos(\phi_{S_b} + \phi_{S_a})} \cos(\phi_{S_a} + \phi_{S_b}) + A_{TT}^{\cos(4\phi - \phi_{S_a} - \phi_{S_b})} \cos(4\phi - \phi_{S_a} - \phi_{S_b}) \right)$$

$$+ A_{TT}^{\cos(2\phi - \phi_{S_a} + \phi_{S_b})} \cos(2\phi - \phi_{S_a} + \phi_{S_b}) + A_{TT}^{\cos(2\phi + \phi_{S_a} - \phi_{S_b})} \cos(2\phi + \phi_{S_a} - \phi_{S_b}) \Big]$$

The azimuthal asymmetries can be calculated as ratios of cross sections differences to the sum of the integrated over \vec{x} cross sections.

The azimuthal distribution of DY pair's produced in non-polarized hadron collisions, A_{UU} , and azimuthal asymmetries of the cross sections in polarized hadron collisions, A_{jk} , are given by relations shown left.



2. Physics motivations.



Nucleon spin structure studies using the Drell-Yan reactions.
The PDFs studies via asymmetry of the Drell-Yan pairs.

Applying the Fourier analysis to the measured asymmetries, one can separate each of all ratios entering previous slide.

This will be the one of task of the experiments proposed for SPD.

The extraction of different TMD PDFs from those ratios is a task of the global theoretical analysis (a challenge for the theoretical community) since each of the SFs a result of convolutions of different TMD PDFs in the quark transverse momentum space.

For this purpose one needs either to assume a factorization of the transverse momentum dependence for each TMD PDFs, having definite mathematic form (usually Gaussian) with some parameters to be fitted

(M. Anselmino et al., arXiv:1304.7691 [hep-ph]),

or to transfer to impact parameter representation space and to use the Bessel weighted TMD PDFs

(Daniel Boer, Leonard Gamberg, Bernhard Musch, Alexei Prokudin, JHEP 1110 (2011) 021, [arXiv:1107.5294])

2. Physics motivations.

Nucleon spin structure studies using the Drell-Yan reactions.
Studies of PDFs via integrated asymmetries.

The set of asymmetries mentioned above gives the access to all eight leading twist TMD PDFs. However, sometimes one can work with integrated asymmetries. Integrated asymmetries are useful for the express analysis of data and checks of expected relations between asymmetries mentioned above. They are also useful for model estimations and determination of required statistics. Let us consider several examples starting from the case when only one of colliding hadrons (for instance, hadron "b") is transversely polarized. In this case the DY cross section can be reduced to the expression:

$$\begin{aligned} \frac{d\sigma}{dx_a dx_b d^2\mathbf{q}_T d\Omega} = & \frac{\alpha^2}{4Q^2} \left\{ (1 + \cos^2 \theta) C \left[f_1 \bar{f}_1 \right] \right. \\ & + \sin^2 \theta \cos 2\phi C \left[\frac{2(\vec{h} \cdot \vec{k}_{aT})(\vec{h} \cdot \vec{k}_{bT}) - \vec{k}_{aT} \cdot \vec{k}_{bT}}{M_a M_b} h_1^\perp \bar{h}_1^\perp \right] \\ & + |S_{bT}| \left[(1 + \cos^2 \theta) \sin(\phi - \phi_{S_b}) C \left[\frac{\vec{h} \cdot \vec{k}_{bT}}{M_b} f_1 \bar{f}_{1T}^\perp \right] - \sin^2 \theta \sin(\phi + \phi_{S_b}) C \left[\frac{\vec{h} \cdot \vec{k}_{aT}}{M_a} h_1^\perp \bar{h}_1 \right] \right. \\ & \left. - \sin^2 \theta \sin(3\phi - \phi_{S_b}) C \left[\frac{2(\vec{h} \cdot \vec{k}_{bT})[2(\vec{h} \cdot \vec{k}_{aT})(\vec{h} \cdot \vec{k}_{bT}) - \vec{k}_{aT} \cdot \vec{k}_{bT}] - \vec{k}_{bT}^2 (\vec{h} \cdot \vec{k}_{aT})}{2M_a M_b^2} h_1^\perp \bar{h}_{1T}^\perp \right] \right] \left. \right\} \end{aligned}$$

2. Physics motivations.

Nucleon spin structure studies using the DY reactions.
Studies of PDFs via integrated asymmetries.

$$A_{UT}^{w[\sin(\phi+\phi_S)]} = \frac{\int d\Omega d\phi_S \sin(\phi+\phi_S) [d\sigma^\uparrow - d\sigma^\downarrow]}{\int d\Omega d\phi_S [d\sigma^\uparrow + d\sigma^\downarrow]/2} = -\frac{1}{2} \frac{C \left[\frac{\vec{h} \cdot \vec{k}_{aT}}{M_a} h_1^\perp \bar{h}_1 \right]}{C [f_1 \bar{f}_1]},$$

$$A_{UT}^{w[\sin(\phi-\phi_S)]} = \frac{\int d\Omega d\phi_S \sin(\phi-\phi_S) [d\sigma^\uparrow - d\sigma^\downarrow]}{\int d\Omega d\phi_S [d\sigma^\uparrow + d\sigma^\downarrow]/2} = \frac{1}{2} \frac{C \left[\frac{\vec{h} \cdot \vec{k}_{bT}}{M_b} f_1 \bar{f}_{1T} \right]}{C [f_1 \bar{f}_1]},$$

$$A_{UT}^{w[\sin(3\phi-\phi_S)]} = \frac{\int d\Omega d\phi_S \sin(3\phi-\phi_S) [d\sigma^\uparrow - d\sigma^\downarrow]}{\int d\Omega d\phi_S [d\sigma^\uparrow + d\sigma^\downarrow]/2} = -\frac{1}{2} \frac{C \left[\frac{2(\vec{h} \cdot \vec{k}_{bT})[2(\vec{h} \cdot \vec{k}_{aT})(\vec{h} \cdot \vec{k}_{bT}) - \vec{k}_{aT} \cdot \vec{k}_{bT}] - \vec{k}_{bT}^2 (\vec{h} \cdot \vec{k}_{aT})}{2M_a M_b^2} h_1^\perp \bar{h}_{1T} \right]}{C [f_1 \bar{f}_1]}$$

$$A_{UT}^{w[\sin(\phi+\phi_S) \frac{q_T}{M_N}]} = \frac{\int d\Omega \int d^2 \mathbf{q}_T (|\mathbf{q}_T|/M_p) \sin(\phi+\phi_S) [d\sigma^\uparrow - d\sigma^\downarrow]}{\int d\Omega \int d^2 \mathbf{q}_T [d\sigma^\uparrow + d\sigma^\downarrow]/2} = -\frac{\sum_q e_q^2 \left[\bar{h}_{1q}^{\perp(1)}(x_p) h_{1q}(x_{p\uparrow}) + (q \leftrightarrow \bar{q}) \right]}{\sum_q e_q^2 \left[\bar{f}_{1q}(x_p) f_{1q}(x_{p\uparrow}) + (q \leftrightarrow \bar{q}) \right]},$$

$$A_{UT}^{w[\sin(\phi-\phi_S) \frac{q_T}{M_N}]} = \frac{\int d\Omega \int d^2 \mathbf{q}_T (|\mathbf{q}_T|/M_p) \sin(\phi-\phi_S) [d\sigma^\uparrow - d\sigma^\downarrow]}{\int d\Omega \int d^2 \mathbf{q}_T [d\sigma^\uparrow + d\sigma^\downarrow]/2} = 2 \frac{\sum_q e_q^2 \left[f_{1T}^{\perp(1)q}(x_{p\uparrow}) f_{1q}(x_p) + (q \leftrightarrow \bar{q}) \right]}{\sum_q e_q^2 \left[\bar{f}_{1q}(x_{p\uparrow}) f_{1q}(x_p) + (q \leftrightarrow \bar{q}) \right]},$$

where

$$h_{1q}^{\perp(1)}(x) = \int d^2 k_T \left(\frac{k_T^2}{2M_p^2} \right) h_{1q}^\perp(x_p, k_T^2) \quad \text{and} \quad f_{1qT}^{\perp(1)}(x) = \int d^2 k_T \left(\frac{k_T^2}{2M_p^2} \right) f_{1qT}^{\perp(1)}(x, k_T^2)$$

The integrated and additionally q_T -weighted asymmetries $A_{UT}^{w[\sin(\phi+\phi_S) \frac{q_T}{M_N}]}$ and $A_{UT}^{w[\sin(\phi-\phi_S) \frac{q_T}{M_N}]}$ provide access to the first moments of the Boer-Mulders, $h_{1q}^\perp(x, k_T^2)$ and Sivers, $f_{1qT}^{\perp(1)}(x, k_T^2)$

$$A_{UT}^{w[\sin(\phi-\phi_S) \frac{q_T}{M_N}]} \Big|_{x_p \gg x_{p\uparrow}} \approx 2 \frac{\bar{f}_{1uT}^{\perp(1)}(x_{p\uparrow})}{\bar{f}_{1u}(x_{p\uparrow})} ; \quad A_{UT}^{w[\sin(\phi+\phi_S) \frac{q_T}{M_N}]} \Big|_{x_p \gg x_{p\uparrow}} \approx -\frac{\bar{h}_{1u}^{\perp(1)}(x_p) \bar{h}_{1u}(x_{p\uparrow})}{\bar{f}_{1u}(x_p) \bar{f}_{1u}(x_{p\uparrow})}$$

$$A_{UT}^{w[\sin(\phi-\phi_S) \frac{q_T}{M_N}]} \Big|_{x_p \ll x_{p\uparrow}} \approx 2 \frac{f_{1uT}^{\perp(1)}(x_{p\uparrow})}{f_{1u}^{\perp(1)}(x_{p\uparrow})} ; \quad A_{UT}^{w[\sin(\phi+\phi_S) \frac{q_T}{M_N}]} \Big|_{x_p \ll x_{p\uparrow}} \approx -\frac{\bar{h}_{1u}^{\perp(1)}(x_p) h_{1u}(x_{p\uparrow})}{\bar{f}_{1u}(x_p) f_{1u}(x_{p\uparrow})}$$

A. Sissakian, O. Shevchenko, A. Nagaytsev, and O. Ivanov, arXiv:0807.2480 [hep-ph].

A. Sissakian, O. Shevchenko, A. Nagaytsev and O. Ivanov, Phys. Rev. D72(2005) 054027), [arXiv:hep-ph/0505214].

A. Sissakian, et al., Eur. Phys. J. C46 (2006)147, [arXiv:hep-ph/0512095].

2. Physics motivations.

Nucleon spin structure studies using the Drell-Yan reactions. Studies of PDFs via integrated asymmetries.

So far the pp -collisions have been considered. At NICA the pd - and dd -collisions will be investigated as well. As it is known from COMPASS experiment, the SIDIS asymmetries on polarized deuterons are consistent with zero. At NICA one can expect that asymmetries

$$A_{UT}^w \left[\sin(\phi \pm \phi_S) \frac{q_T}{M_N} \right] \Bigg|_{pD^\uparrow}, \quad A_{UT}^w \left[\sin(\phi \pm \phi_S) \frac{q_T}{M_N} \right] \Bigg|_{DD^\uparrow} \quad \text{also will be consistent with zero (subject of tests).}$$

But asymmetries in Dp^\uparrow collisions are expected to be non-zero. In the limiting cases $x_D \gg x_{p^\uparrow}$ and $x_D \ll x_{p^\uparrow}$ these asymmetries (**accessible only at NICA**)

$$A_{UT}^w \left[\sin(\phi - \phi_S) \frac{q_T}{M_N} \right] (x_D \gg x_{p^\uparrow}) \Bigg|_{Dp^\uparrow \rightarrow I^+ I^- X} \approx \frac{4 \bar{f}_{lu}^{\perp(1)}(x_{p^\uparrow}) + \bar{f}_{ld}^{\perp(1)}(x_{p^\uparrow})}{4 \bar{f}_{lu}^{\perp(1)}(x_{p^\uparrow}) + \bar{f}_{ld}^{\perp(1)}(x_{p^\uparrow})},$$

$$A_{UT}^w \left[\sin(\phi - \phi_S) \frac{q_T}{M_N} \right] (x_D \ll x_{p^\uparrow}) \Bigg|_{Dp^\uparrow \rightarrow I^+ I^- X} \approx 2 \frac{4 f_{lu}^{\perp(1)}(x_{p^\uparrow}) + f_{ld}^{\perp(1)}(x_{p^\uparrow})}{4 f_{lu}^{\perp(1)}(x_{p^\uparrow}) + f_{ld}^{\perp(1)}(x_{p^\uparrow})},$$

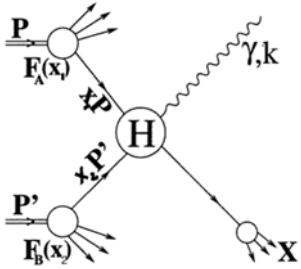
$$A_{IT}^w \cos(\phi_{Sb} + \phi_{Sa}) q_T / M \equiv A_{IT}^{\text{int}} = \frac{\sum_q e_q^2 (\bar{h}_{1q}(x_1) h_{1q}(x_2) + (x_1 \leftrightarrow x_2))}{\sum_q e_q^2 (\bar{f}_{1q}(x_1) f_{1q}(x_2) + (x_1 \leftrightarrow x_2))}.$$

$$A_{UT}^w \left[\sin(\phi + \phi_S) \frac{q_T}{M_N} \right] (x_D \gg x_{p^\uparrow}) \Bigg|_{Dp^\uparrow \rightarrow I^+ I^- X} \approx - \frac{[h_{lu}^{\perp(1)}(x_D) + h_{ld}^{\perp(1)}(x_D)][4 \bar{h}_{lu}(x_{p^\uparrow}) + \bar{h}_{ld}(x_{p^\uparrow})]}{[f_{lu}(x_D) + f_{ld}(x_D)][4 \bar{f}_{lu}(x_{p^\uparrow}) + \bar{f}_{ld}(x_{p^\uparrow})]},$$

$$A_{UT}^w \left[\sin(\phi + \phi_S) \frac{q_T}{M_N} \right] (x_D \ll x_{p^\uparrow}) \Bigg|_{Dp^\uparrow \rightarrow I^+ I^- X} \approx - \frac{[\bar{h}_{lu}^{\perp(1)}(x_D) + \bar{h}_{ld}^{\perp(1)}(x_D)][4 h_{lu}(x_{p^\uparrow}) + h_{ld}(x_{p^\uparrow})]}{[\bar{f}_{lu}(x_D) + \bar{f}_{ld}(x_D)][4 f_{lu}(x_{p^\uparrow}) + f_{ld}(x_{p^\uparrow})]}.$$

2. Physics motivations.

Direct photons.



Prompt photons produced in pp interaction

Access to gluon polarization via DLSA: $A_{LL} = \frac{(\sigma_{++} + \sigma_{--}) - (\sigma_{+-} + \sigma_{-+})}{(\sigma_{++} + \sigma_{--}) + (\sigma_{+-} + \sigma_{-+})}$

$$A_{LL} \sim \frac{\Delta g(x_1)}{g(x_1)} \cdot \left[\frac{\sum_q e_q^2 [\Delta q(x_2) + \Delta \bar{q}(x_2)]}{\sum_q e_q^2 [q(x_2) + \bar{q}(x_2)]} \right] + [x_1 \leftrightarrow x_2]$$

$A_{1,p,D,\dots}$ well known

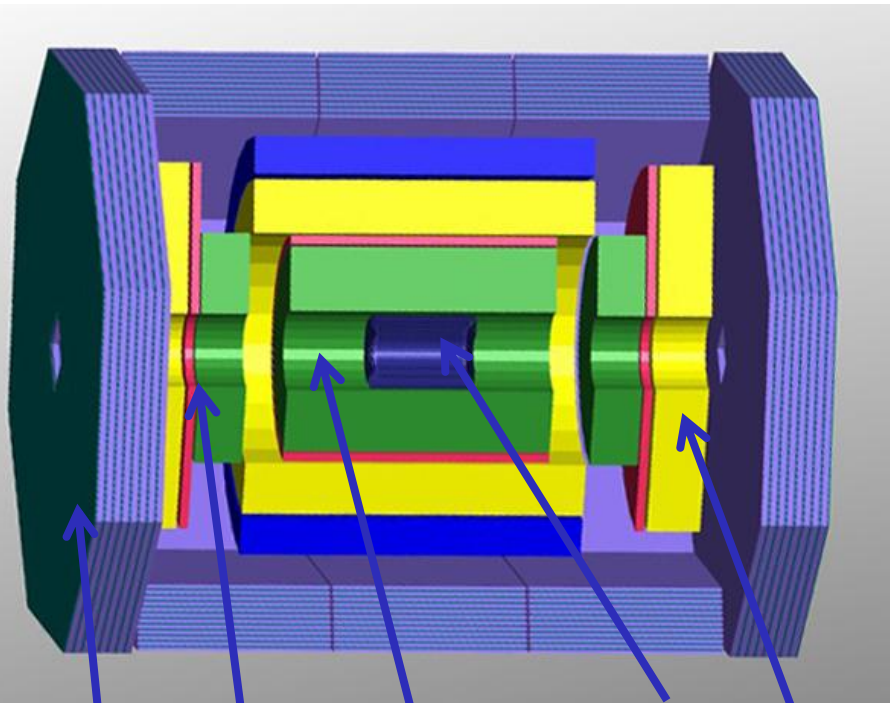
Access to gluon Sivers function via STSA:

$$A_N = \frac{\sigma^\uparrow - \sigma^\downarrow}{\sigma^\uparrow + \sigma^\downarrow}$$

$$\sigma^\uparrow - \sigma^\downarrow = \sum_i \int_{x_{min}}^1 dx_a \int d^2 \mathbf{k}_{Ta} d^2 \mathbf{k}_{Tb} \frac{x_a x_b}{x_a - (p_T/\sqrt{s})} e^y [q_i(x_a, \mathbf{k}_{Ta}) \Delta_N G(x_b, \mathbf{k}_{Tb}) \times \frac{d\hat{\sigma}}{d\hat{t}}(q_i G \rightarrow q_i \gamma) + G(x_a, \mathbf{k}_{Ta}) \Delta_N q_i(x_b, \mathbf{k}_{Tb}) \frac{d\hat{\sigma}}{d\hat{t}}(G q_i \rightarrow q_i \gamma)]$$

Never measured

2. Preliminary SPD design.



The main systems of SPD are:

- magnet (solenoid vs torroid)
- vertex detector (silicon)
- central tracker (straw tubes)
- trigger system (RPC, scint. Counters)
- ECAL
- muon system (range system)

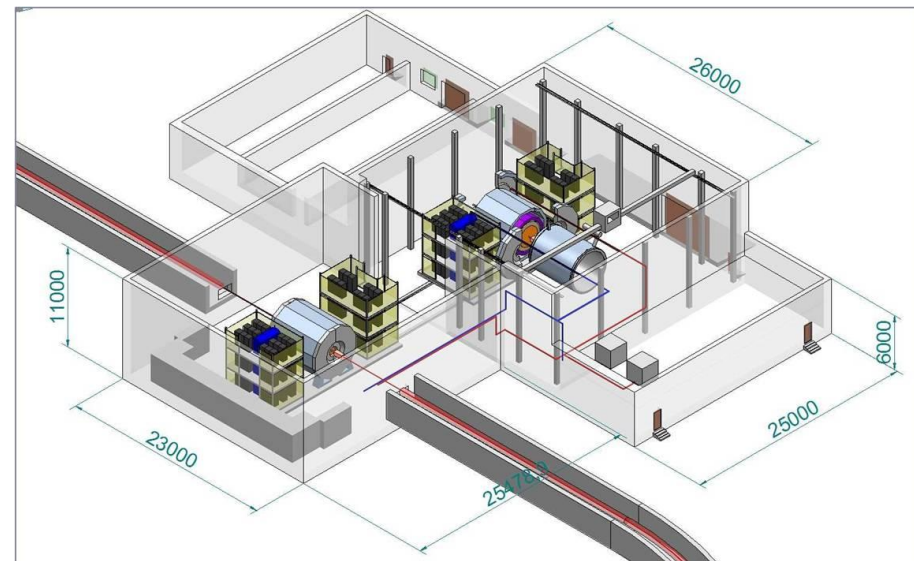
Muon system

Vertex detector

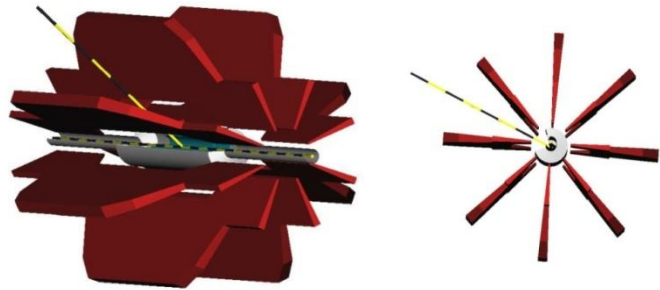
Central tracker,
straw tubes

ECAL

RPC/TOF

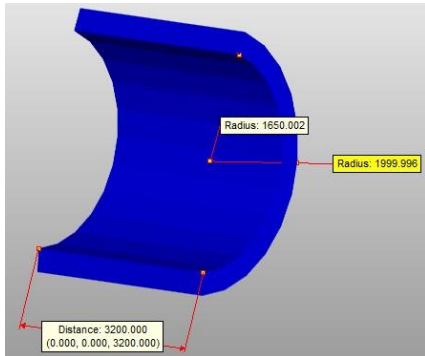


2. Preliminary SPD design.



Magnet: toroid vs. solenoid

One can consist of 8 superconducting coils symmetrically placed around the beam axis. Preliminary studies show that the use of superconducting coils, allows one to reach an azimuthal detector acceptance of about 85%.

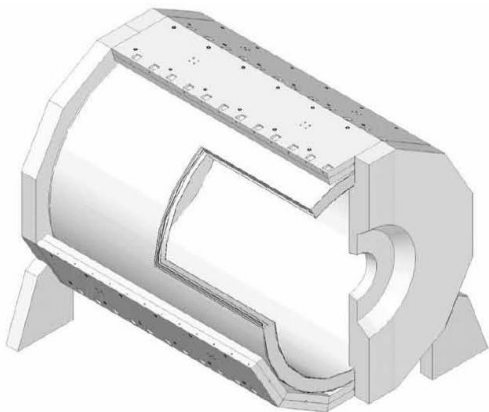


No field in beam pipe.

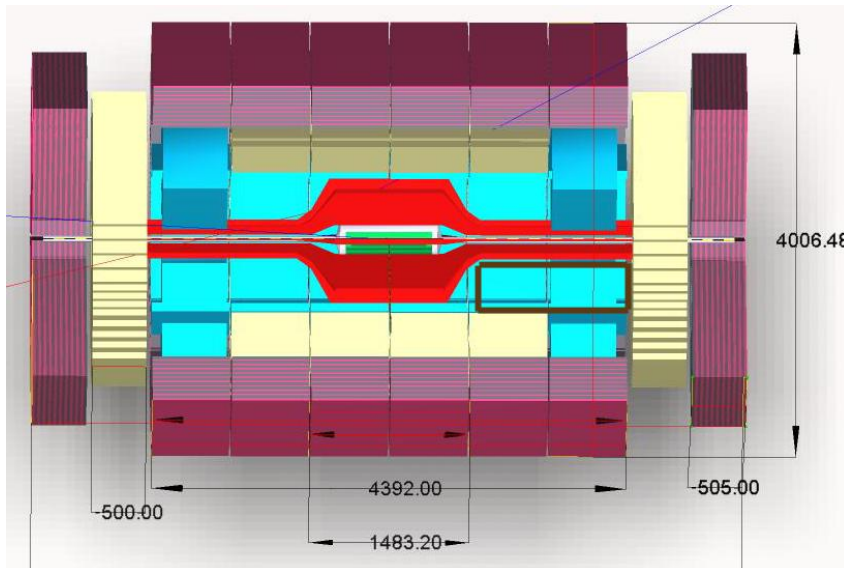
Solenoid:

The maximum magnetic field of $\sim 1\text{T}$ over a length of about 3.2m and a diameter of 1.8m. The field homogeneity is foreseen to be better than 1% over the volume of the vertex detector and central tracker.

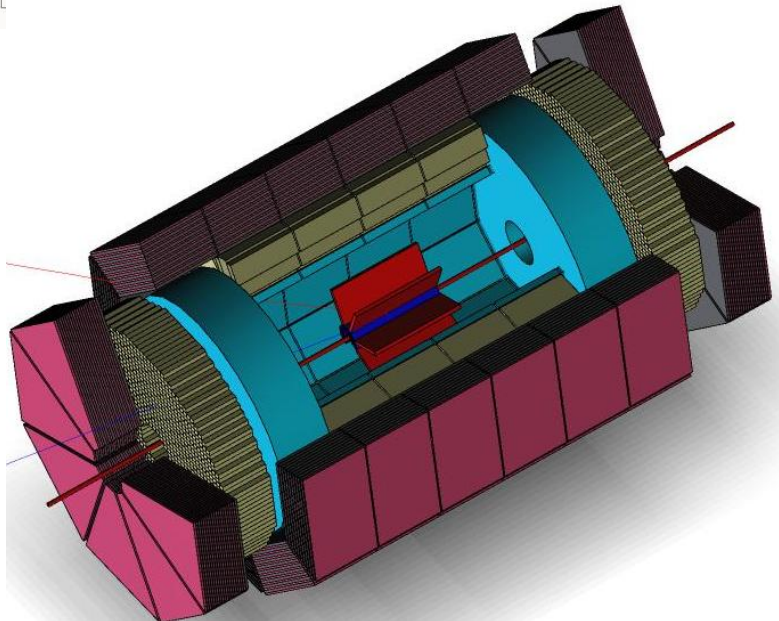
Need to have the special magnetic shield for transverse polarized beams.



3. SPD with Torroid magnet

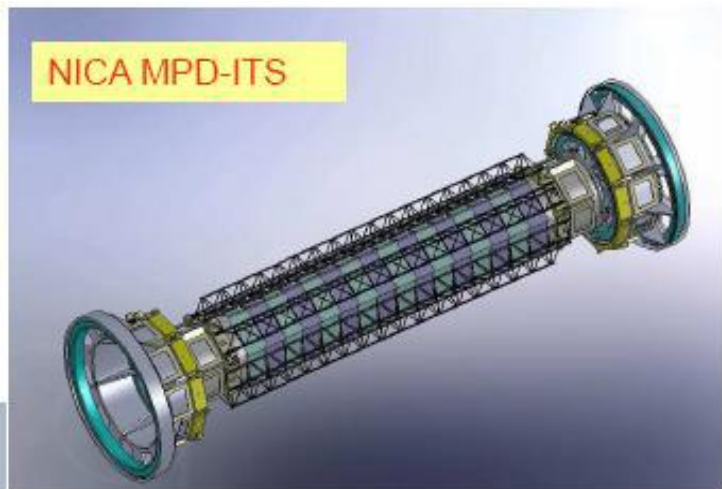


The torroid magnet can consist of 8 superconducting coils symmetrically placed around the beam axis. A support ring upstream (downstream) of the coils hosts the supply lines for electric power and for liquid helium. At the downstream end, a hexagonal plate compensates the magnetic forces to hold the coils in place. The field lines of ideal toroid magnet are always perpendicular to the particles originating from the beam intersection point. Since the field intensity increases inversely proportional to the radial distance: greater bending power is available for particles scattering at smaller angles and having higher momenta. These properties help to design a compact spectrometer that keeps the investment costs for the detector tolerable. The production of such a magnet requires insertion of the coils into the tracking volume occupying a part of the azimuthal acceptance.



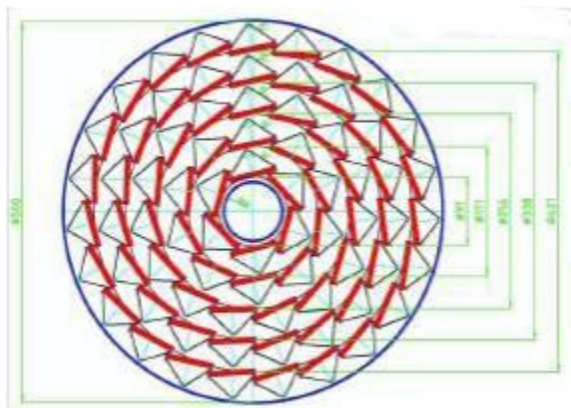
No field in beam pipe.

Two options are possible:
"warm" torroid and "cold" torroid.

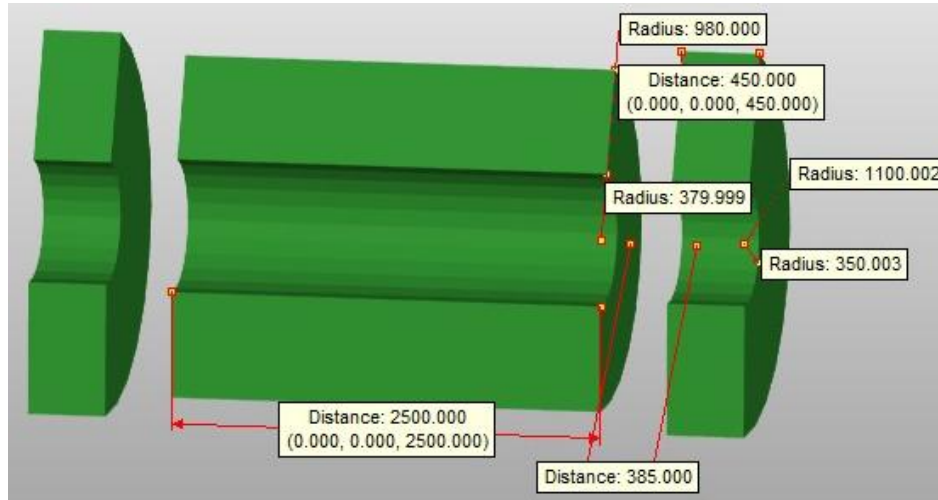


Silicon Microvertex Detector

The most obvious technology for the vertex detector (VD) is a silicon one (see pictures). It is approved for the MPD VD. Outside the beam pipe. Several layers of double-sided silicon strips can provide a precise vertex reconstruction and tracking of the particles before they reach the general SPD tracking system. The design should use a small number of silicon layers to minimize the radiation length of the material. With a pitch of 50-100 μm it is possible to reach the spatial resolution of 20-30 μm . Such a spatial resolution would provide 50-80 μm for precision of the vertex reconstruction. This permits to reject the secondary decay vertexes.



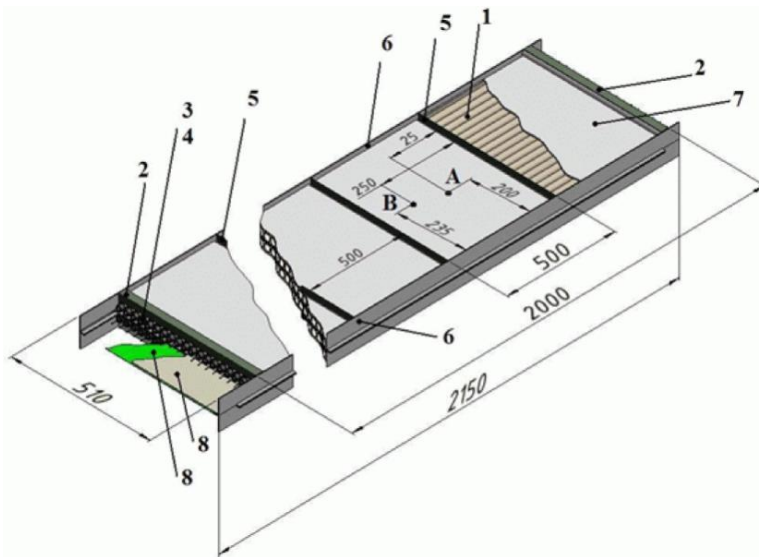
2. Preliminary SPD design.



The straw tubes can be selected to be the main detector of SPD Tracking System. This choice is due to the following properties of the straws tubes:

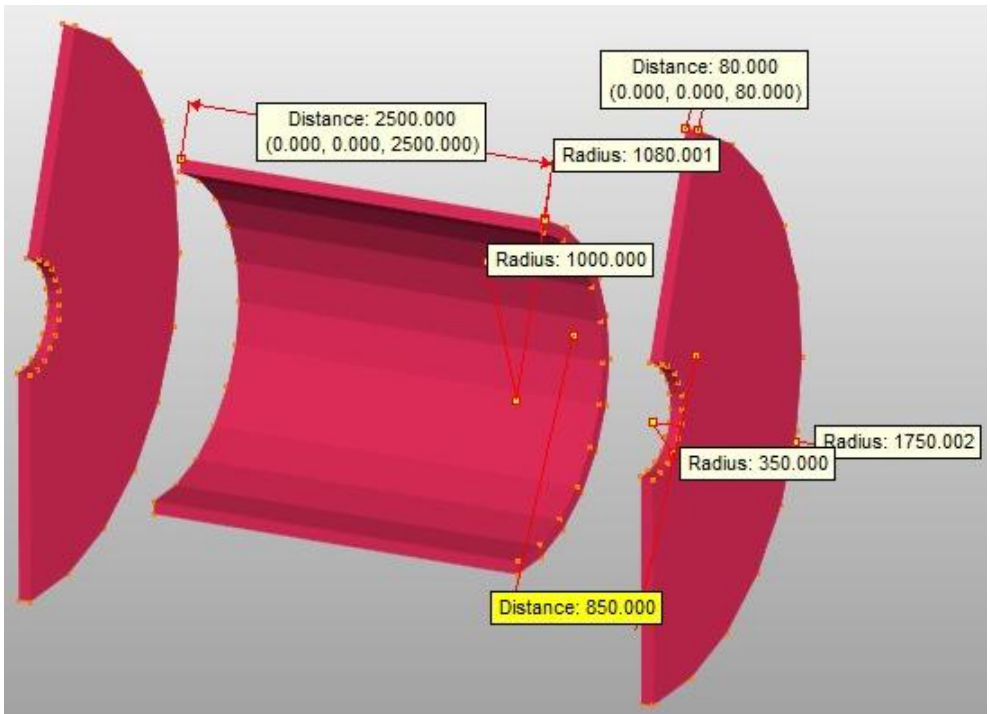
- the minimum of material for the tracks of the secondary particles ($X_0 \sim 0.1$);
- the time (~ 200 - 300 ns) and spatial (track resolution ~ 100 μm);
- expected particle rates (DAQ rates ~ 100 KHz);
- the developed production sites (also in JINR, Dubna).

The one the main point of straw system development is the requirements of the minimization of material budget. To meet this requirement it is planned to use the thin-walled tubes.



- V.A. Baranov et al, Instrum. Exp. Tech. 55 (2012) 26-28
- Bazylev S.N. et al., JINR Preprint P13-2010-60
- Davkov K.I. et al., JINR Preprint P13-2012-93
- NA-62 Collaboration, Technical Design Document, NA62-10-07, December 2010

2. Preliminary SPD design.



The main task of the trigger system is to provide separation of a particular reaction from all reactions occurred in collisions.

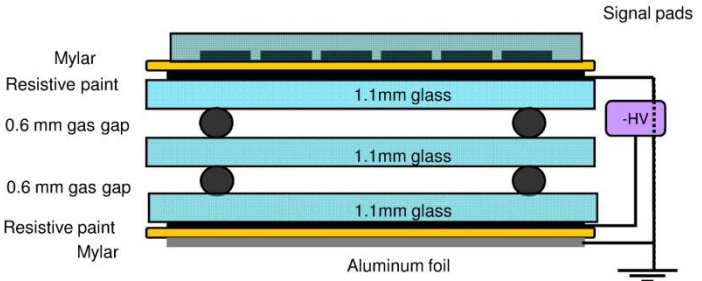
- Each of them will be pre-scaled with:
- two muons (or electrons/positrons) in final states;
 - various types of hadrons in final states ($\pi^{+/-}$, K, p, ...);
 - photons (π^0 , ω , η ...);
 - other reactions.

RPC are proposed to be used as main trigger detector.

Also Hodoscopes of scintillating counters can be used for triggering.

They can be located before and after RS (or mounted in the last layers of RS) and before RPC.

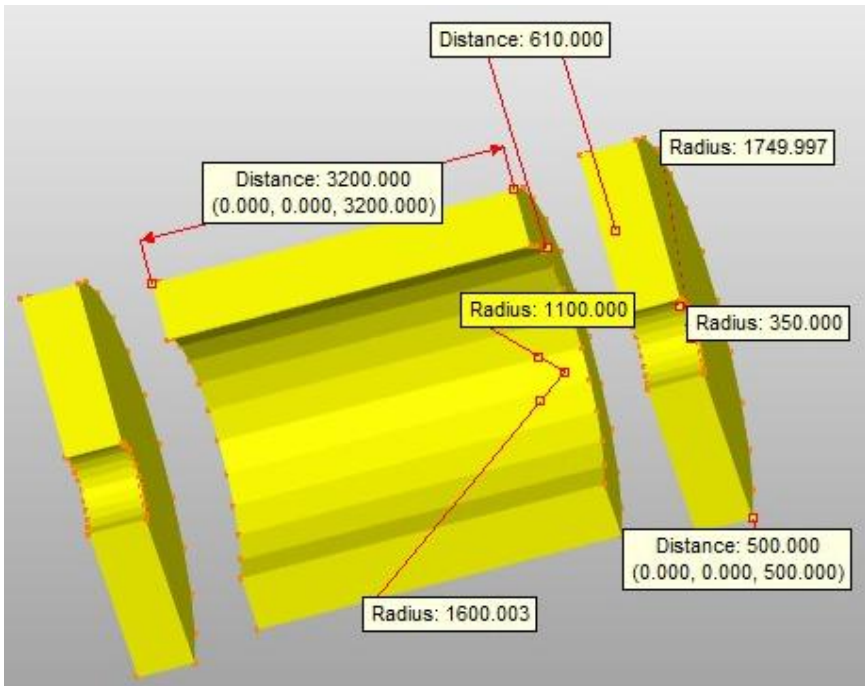
The ECAL modules will also be used in the trigger system.



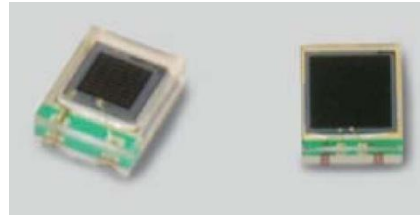
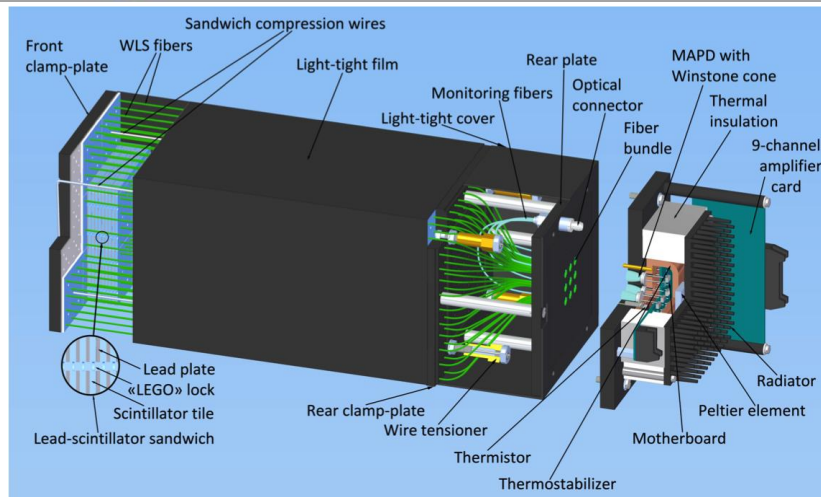
- No wires;
- High efficiency;
- Fast response;
- Position measurement;
- Low production cost;
- Large surface

RPC developed in the 1980's.
 Applied in many experiments:
 ATLAS and CMS (muon systems)
 ALICE (TOF and muon system)
 PHENIX (TOF, muon system);
 OPERA (neutrino detector)

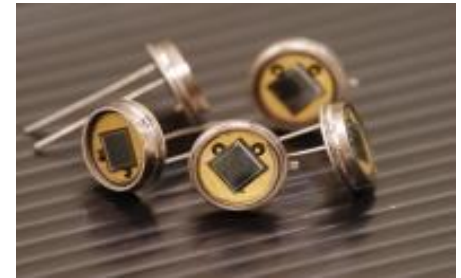
2. Preliminary SPD design.



Photon energy range 0.1- 10GeV.
 Taking into account the space limitation in the barrel region, the total length of module of the ECAL should be less than 50 cm. The required energy resolution $< 10.0\%/\sqrt{E}$ (GeV). The latest version of the electromagnetic calorimeter (ECAL) modules, developed at JINR for the COMPASS-II experiment at CERN, can be good candidates for ECAL at SPD. These "shashlyk" type of modules utilise new photon detectors Avalanche Multichannel Photon Detectors (AMPD). AMPD can work in the strong magnetic field.



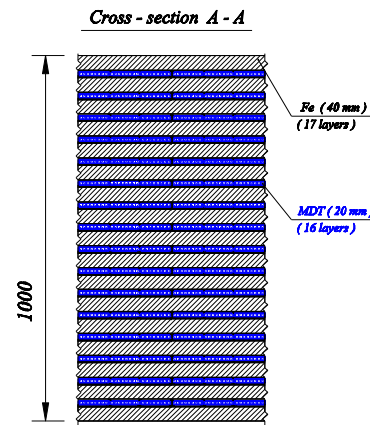
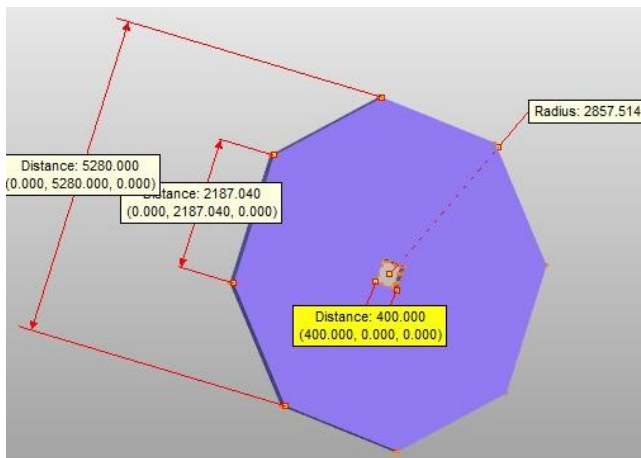
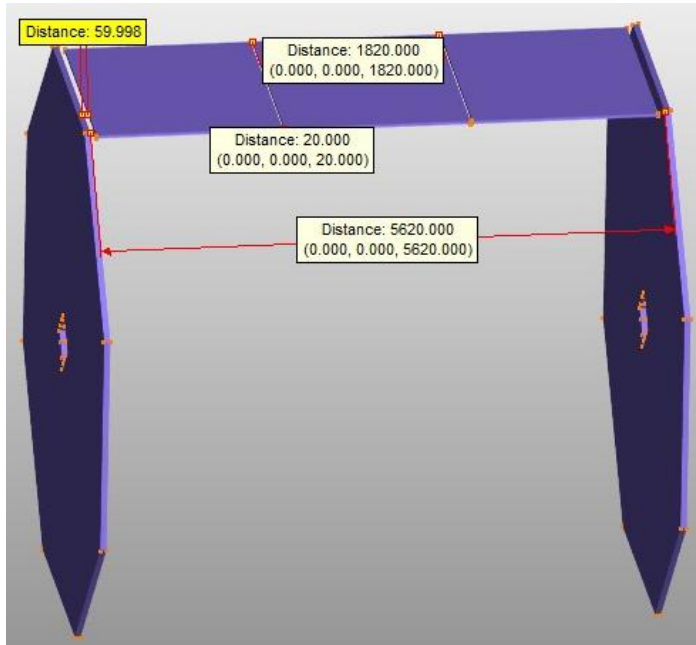
Surface mount type



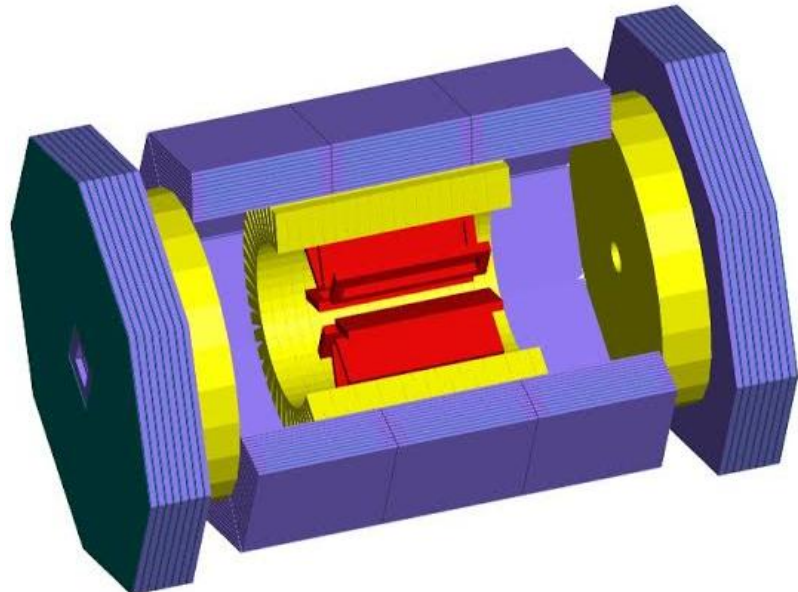
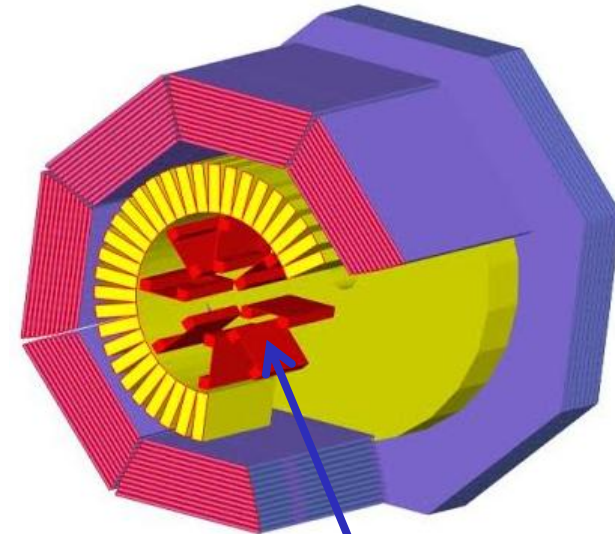
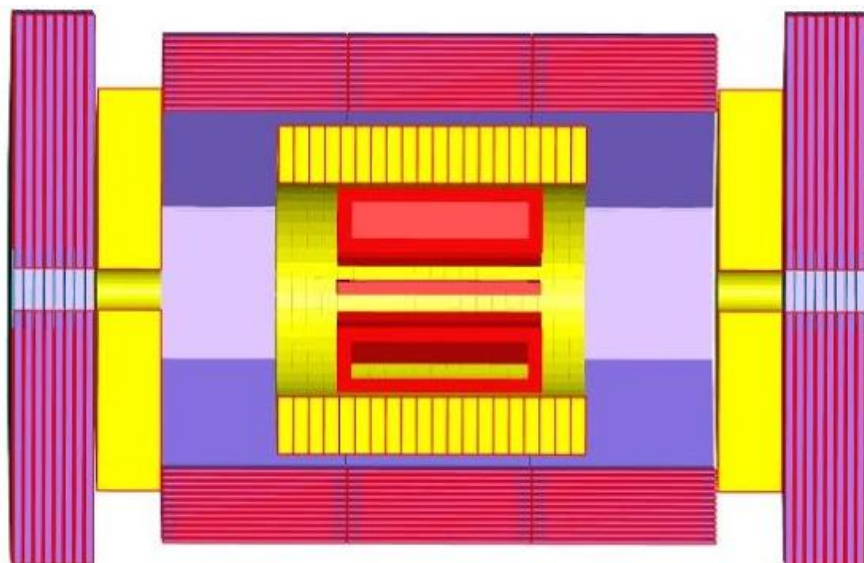
Custom made

2. Preliminary SPD design.

The muon system which uses range system (RS) technique to register muons in laminated iron absorber and is aimed for identifying the primary muons and their separation from background contamination originated mostly from primary low-momenta pions and decay muons. The RS structure is a well known solution for both, detecting the muons stopped by the absorber and those crossing the iron.



3. SPD with Torroid magnet



The torriod magnet can be designed with coordinate detectors located between coils. One can be straw tubes of mini-drift chambers. This system can be used to minimize the background for DY measurements and to improve the accuracy of the particle kinematical variables measurements.



4. Proposed measurements.



We propose to perform measurements of asymmetries of the DY pair's production in collisions of polarized protons and deuterons which provide an access to all collinear and TMD PDFs of quarks and anti-quarks in nucleons.

The measurements of asymmetries in production of J/ψ and direct photons will be performed simultaneously with DY using dedicated triggers.

The set of these measurements will supply complete information for tests of the quark-parton model of nucleons at the twist-two level with minimal systematic errors.

4. Proposed measurements.

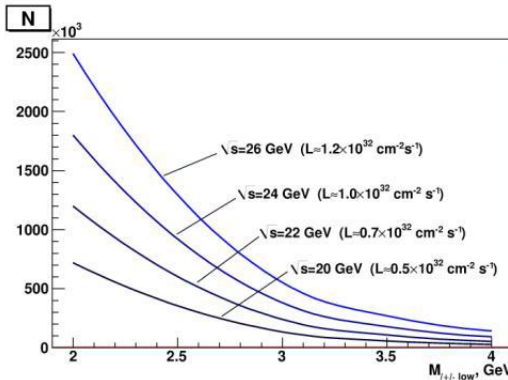
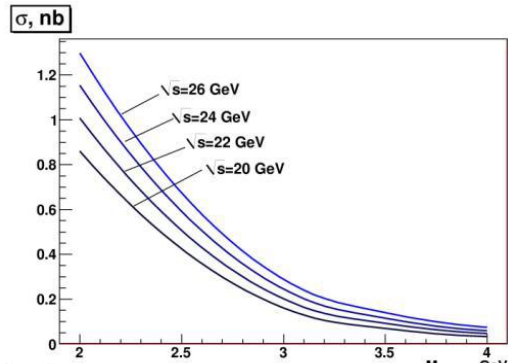
Estimations of DY pairs and J/Ψ production rates.

Estimation of the DY pair's production rate at SPD was performed using the expression for the differential and total cross sections of the pp interactions:

$$\frac{d^2\sigma}{dQ^2 dx_1} = \frac{1}{sx_1} \frac{4\pi\alpha^2}{9Q^2} \sum_{f,\bar{f}} e_f^2 [f(x_1, Q^2) \bar{f}(x_2, Q^2)]_{x_2=Q^2/sx_1}$$

$$\sigma_{tot} = \int_{Q_{min}^2}^{Q_{max}^2} dQ^2 \int_{x_{min}}^1 dx_1 \frac{d^2\sigma}{dQ^2 dx_1},$$

The Table shows values of the cross sections and expected statistics for DY events (K events) per four moths of data taking and 100% acceptance of SPD at two energies.



Cross section (left) and number of DY events (right) versus the minimal invariant mass of lepton pair for various proton beam energies

Lower cut on M_{l+l-} , GeV	2.0	3.0	3.5	4.0
$\sqrt{s}=24$ GeV ($L = 1.0 \cdot 10^{32} \text{ cm}^{-2} \text{ s}^{-1}$)				
$\sigma_{\text{DY total}}$, nb	1.15	0.20	0.12	0.06
events	1800	313	179	92
$\sqrt{s}=26$ GeV ($L = 1.2 \cdot 10^{32} \text{ cm}^{-2} \text{ s}^{-1}$)				
$\sigma_{\text{DY total}}$, nb	1.30	0.24	0.14	0.07
events	2490	460	269	142



4. Proposed measurements.



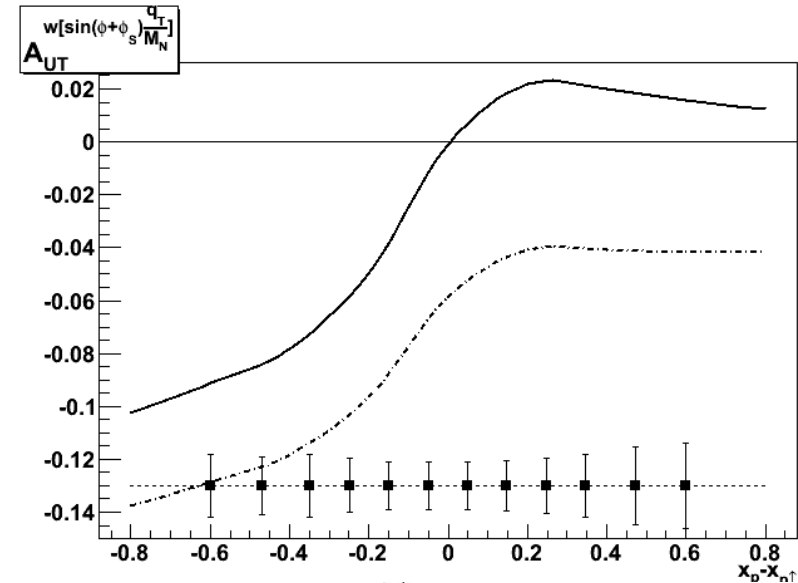
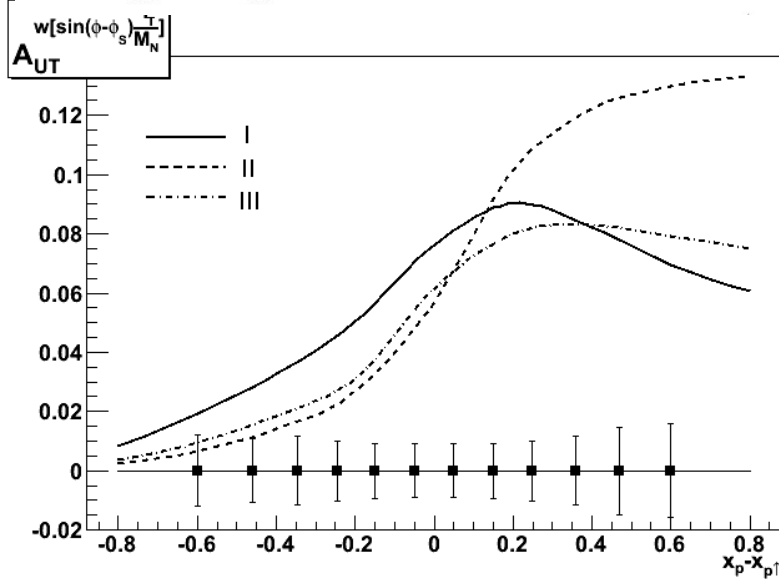
Estimations of DY pairs and J/Ψ production rates.

To estimate the precision of measurements, the set of original software packages for MC simulations, including generators for Sivvers, Boer-Mulders and Transversity PDFs, were developed in

A.Sissakian, O.Shevchenko, A.Nagaytsev, O.Ivanov, Phys.Part.Nucl.41 (2010) 64-100. With these packages a sample of 100K DY events was generated in the region of $Q^2 > 11 \text{ GeV}^2$ for comparison with expected asymmetries.

Fit I: $xf_{1uT}^{\perp(1)} = -xf_{1dT}^{\perp(1)} = 0.4x(1-x)^5$; Fit II: $xf_{1uT}^{\perp(1)} = -xf_{1dT}^{\perp(1)} = 0.1x^{0.3}(1-x)^5$

Fit III: $xf_{1uT}^{\perp(1)} = -xf_{1dT}^{\perp(1)} = (0.17...0.18)x^{0.66}(1-x)^5$



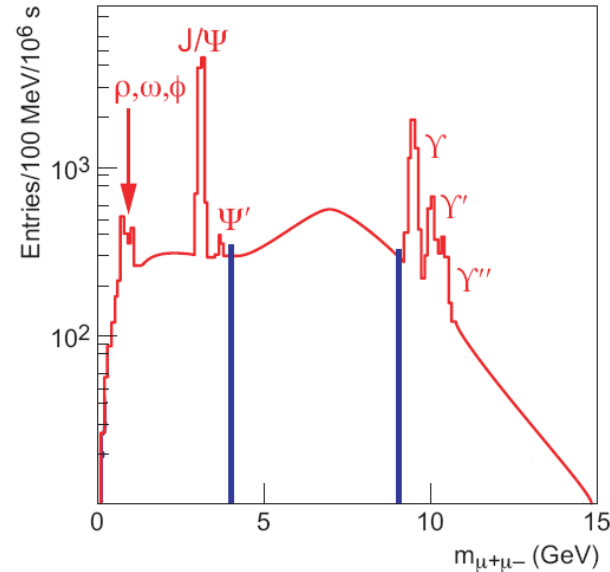
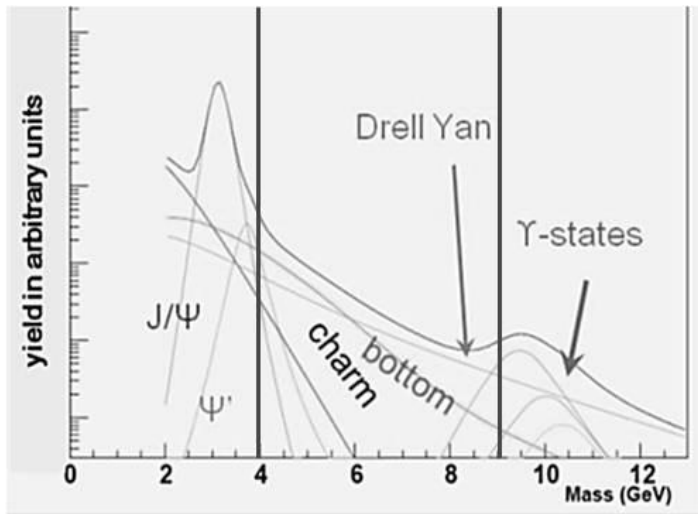
Estimations of Boer-Mulders asymmetry $A_{UT}^w[\sin(\phi+\phi_s) \frac{q_T}{M_N}]$ at $\sqrt{s} = 26 \text{ GeV}$ and $Q^2 = 15 \text{ GeV}^2$. The solid and dotted curves correspond to the first and second versions of the evolution model, respectively. Points with bars show the expected statistical errors obtained with 100K of events

Estimated Sivvers asymmetry $A_{UT}^w[\sin(\phi-\phi_s) \frac{q_T}{M_N}]$ at $\sqrt{s} = 26 \text{ GeV}$ with $Q^2 = 15 \text{ GeV}^2$.

4. Proposed measurements.

Estimations of DY pairs and J/Ψ production rates.

Statistics of the J/Ψ and DY events (with cut on $M_{l-l} = 4 \text{ GeV}$) expected to be recorded (“per year”) in four months of data taking with 100% efficiency of SPD are given in Table.



\sqrt{s} , GeV	24	26	\sqrt{s} , GeV	24	26
$\sigma_{J/\Psi} \cdot B_{e^+e^-}$, nb	12	16	σ_{DY} , nb	0.06	0.07
Events “per year”	$18 \cdot 10^6$	$23 \cdot 10^6$	Events “per year”	$92 \cdot 10^3$	$142 \cdot 10^3$



4. Proposed measurements.



Estimations of direct photon production rates.

Estimation of the direct photon production rates based on PYTHIA6 Monte-Carlo simulation for two values of colliding proton energies. Event rates are given for all and for leading processes of direct photon production considered in PYTHIA.

Statistical accuracies of A_N and A_{LL} measurements at NICA, have been estimated assuming the beam polarizations (both transversal and longitudinal) equal to $P = \pm 0.8$ and overall detector efficiency (acceptance, efficiency of event reconstruction and selection criteria) of about 50%.

To minimize systematic uncertainties, precision of luminosity and beam polarization should be under control, as well as accuracy of π^0 and other background rejection.

$\sqrt{s}=24 \text{ GeV}$ $L = 1.0 \times 10^{32}, \text{ cm}^{-1}\text{s}^{-1}$	$\sigma_{tot},$ nbarn	$\sigma_{P_T > 4 \text{ GeV}/c},$ nbarn	Events/year, 10^6	Events/year, $10^6 (P_T > 4 \text{ GeV}/c)$
All processes	1290	42	3260	105
$qg \rightarrow q\gamma$	1080	33	2730	84
$q\bar{q} \rightarrow g\gamma$	210	9	530	21
$\sqrt{s}=26 \text{ GeV}$ $L = 1.2 \times 10^{32}, \text{ cm}^{-1}\text{s}^{-1}$	$\sigma_{tot},$ nbarn	$\sigma_{P_T > 4 \text{ GeV}/c},$ nbarn	Events/year, 10^6	Events/year, $10^6 (P_T > 4 \text{ GeV}/c)$
All processes	1440	48	4340	144
$qg \rightarrow q\gamma$	1220	38	3680	116
$q\bar{q} \rightarrow g\gamma$	240	10	660	28

5. Future DY experiments

The SPD experiments will have a number of advantages for DY measurements related to nucleon structure studies. These advantages include:

- operations with pp, pd and dd beams,
- scan of effects on beam energies,
- measurement of effects via muon and electron-positron pairs simultaneously,
- operations with non-polarized, transverse and longitudinally polarized beams or their combinations.

Such possibilities permit for the first time to perform comprehensive studies of all leading twist PDFs of nucleons in a single experiment with minimum systematic errors.

Experiment	CERN, COMPASS-II	FAIR, PANDA	FNAL, E-906	RHIC, STAR	RHIC-PHENIX	NICA, SPD
mode	fixed target	fixed target	fixed target	collider	collider	collider
Beam/target	π^- , p	anti-p,p	π^- , p	pp	pp	pp, pD,DD
Polarization: beam, target	0; ~ 0.8	0; 0	0; 0;	0.5 ; 0.5	0.5 ; 0.5	0.5 ; 0.5
Luminosity, $\text{cm}^{-2}\text{s}^{-1}$	10^{32}	10^{32}	10^{42}	10^{32}	10^{32}	10^{32}
\sqrt{s} , GeV	17	6	16	200	200	10-26
$X_{1(\text{beam})} X_{2(\text{targ})}$ ranges	0.1-1.0 ; 0.5-0.9	0.1-1.0 ; 0.3-0.8	0.1-1.0 ; 0.3-0.8	0.1-0.9 ; 0.1-0.9	0.1-0.9 ; 0.1-0.9	0.1-0.8 ; 0.1-0.8
q_T , GeV	0.5 -4.0	0.5 -1.5	0.5 -3.0	1.0 -10.0	1.0 -10.0	0.5 -6.0
Lepton pairs,	$\mu-\mu^+$	$\mu-\mu^+$	$\mu-\mu^+$	$\mu-\mu^+$	$\mu-\mu^+$	$\mu-\mu^+$, e^+e^-
Data taking	2014	>2018	2013	>2016	>2016	>2017
Transversity PDF	YES	NO	NO	YES	YES	YES
Boer-Mulders PDF	YES, valence, $h_{1(\pi)}^+ \otimes h_{1(p)}^+$	YES	YES	YES	YES	YES
Sivers PDF	YES, π PDF	YES	YES	YES	YES	YES
Pretzelocity PDF	YES	NO	NO	NO	YES	YES
Worm Gear PDFs	YES	NO	NO	NO	NO	YES
Duality, J/ Ψ	YES	YES	NO	NO	NO	YES
Flavour decomposition	NO	NO	YES	NO	NO	YES
Lam-Tung relation	NO	NO	NO	NO	NO	YES

We propose to perform measurements of asymmetries of the DY pair's production in collisions of non-polarized, longitudinally and transversally polarized protons and deuterons which provide an access to all leading twist collinear and TMD PDFs of quarks and anti-quarks in nucleons.

The measurements of asymmetries in production of J/Ψ and direct photons will be performed as well simultaneously with DY using dedicated triggers. The set of these measurements will supply complete information for tests of the quark-parton model of nucleons at the QCD twist-two level with minimal systematic errors.

Letter of Intent was approved at the meeting of the JINR Program Advisory Committee (PAC) for Particle Physics on 25-26 June 2014.)

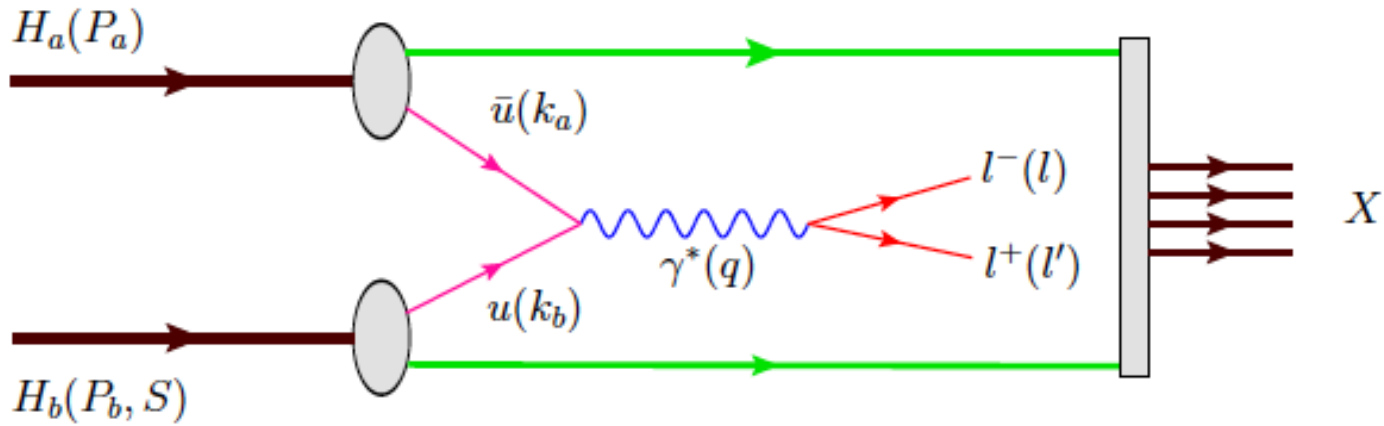
**Collaborators are
welcomed !**





Backup slides.

Drell-Yan Process



$$s = (P_a + P_b)^2,$$

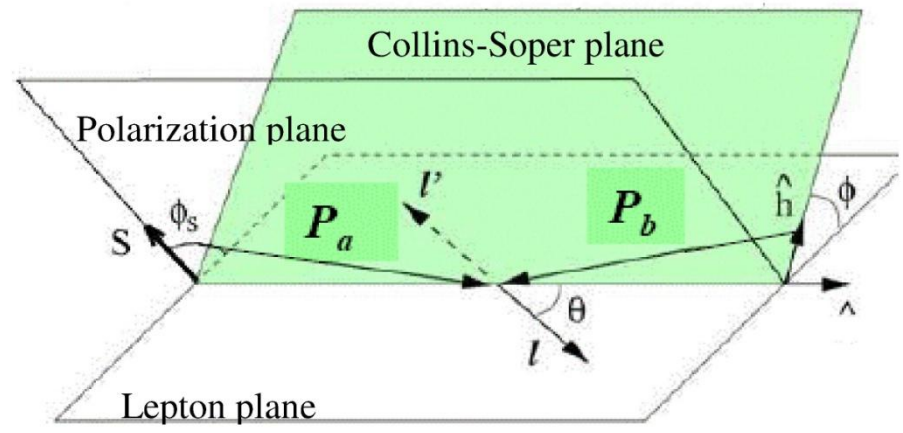
$$x_{a(b)} = q^2 / (2P_{a(b)} \cdot q),$$

$$x_F = x_a - x_b,$$

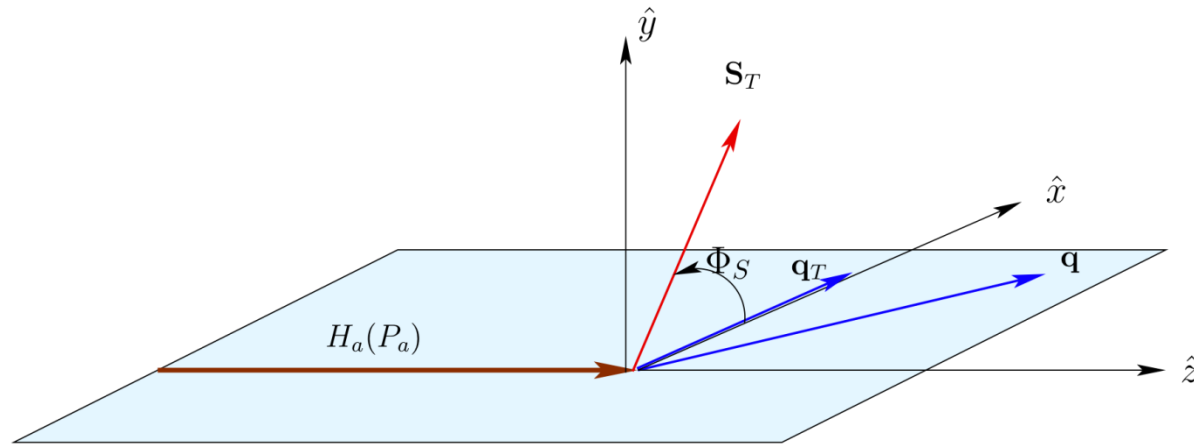
$$M_{\mu\mu}^2 = Q^2 = q^2 = s x_a x_b,$$

$$q_T = P_T = k_{T_a} + k_{T_b}$$

the momentum of the beam (target) hadron,
 the total centre-of-mass energy squared,
 the momentum fraction carried by a parton from $H_{a(b)}$,
 the Feynman variable,
 the invariant mass squared of the dimuon,
 the transverse component of the quark momentum,
 the transverse component of the momentum of the virtual photon.

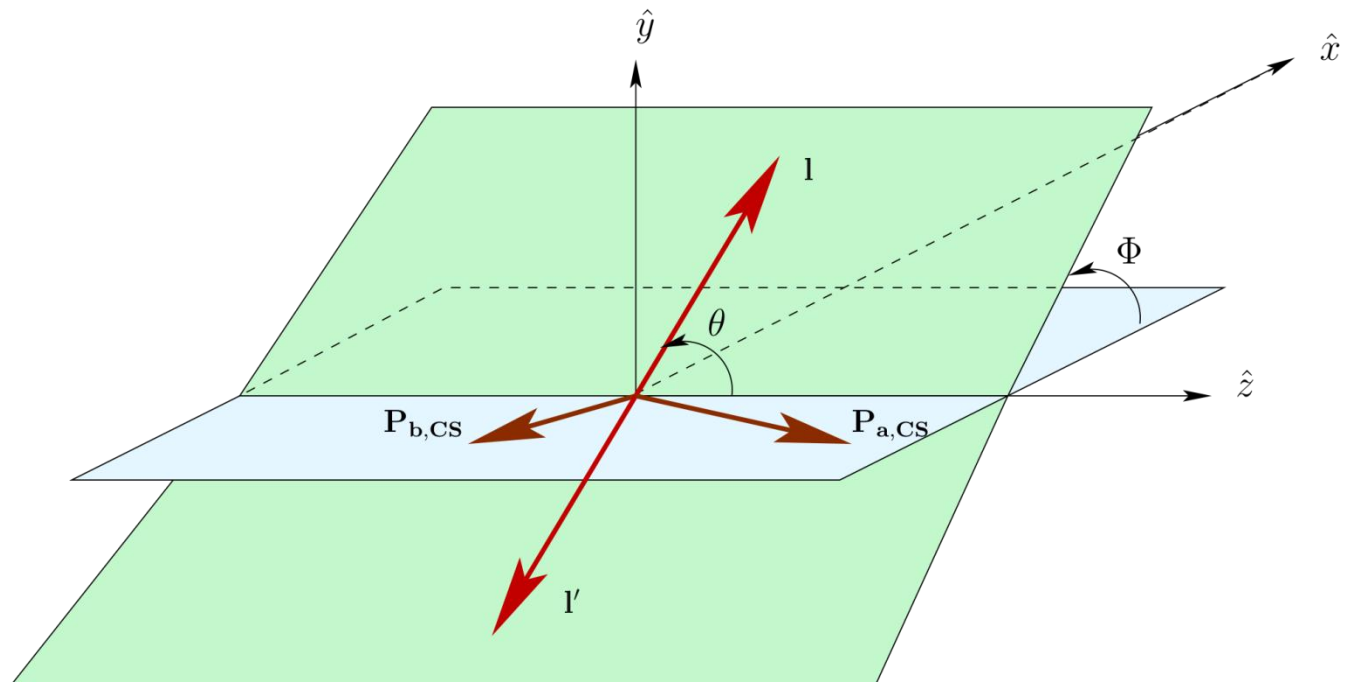


Coordinate systems



TF

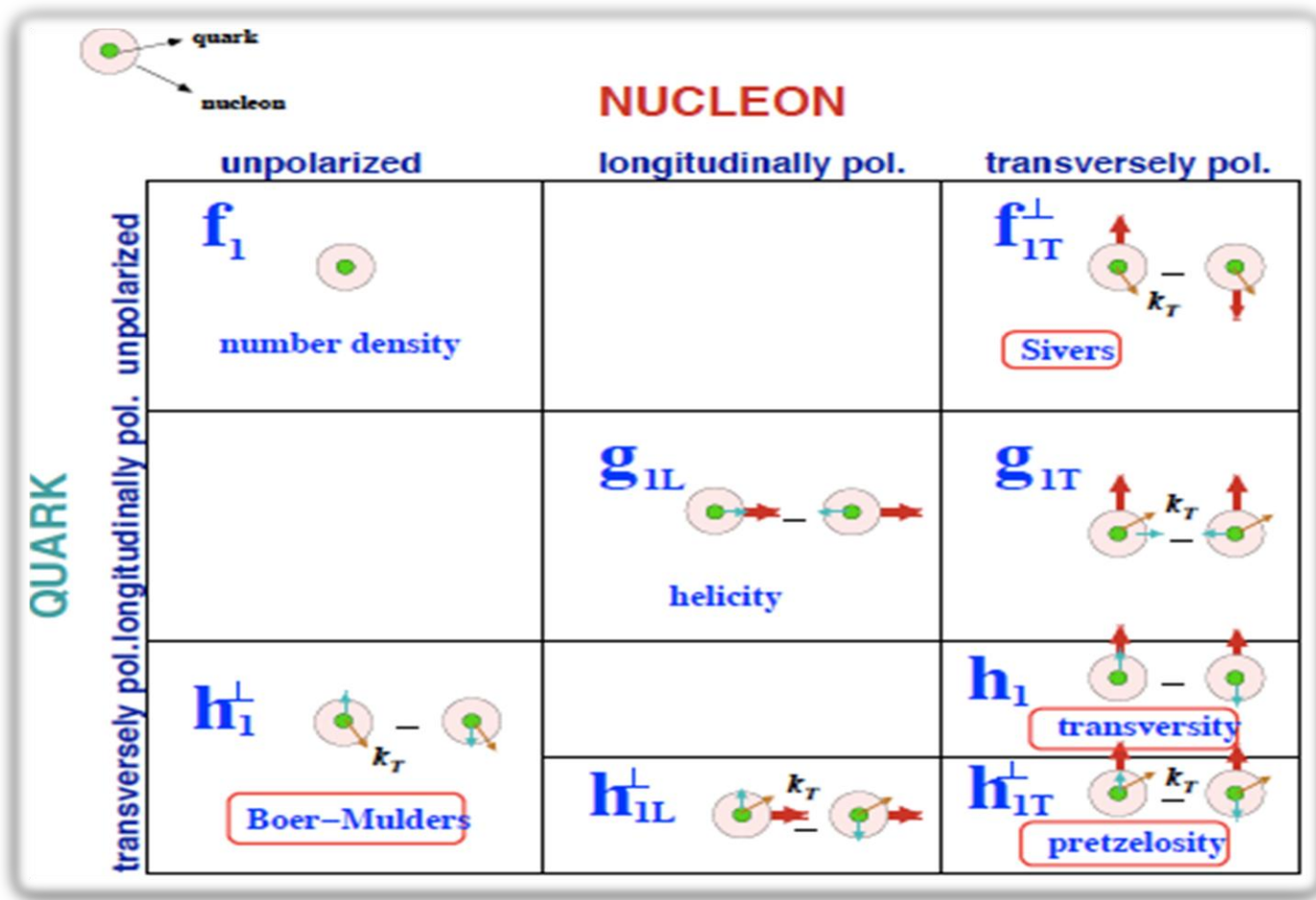
Collins-Soper



LEADING ORDER PDFs

At leading order, 3 PDFs are needed to describe the structure of the nucleon in the collinear approximation.

But if one takes into account also the quarks intrinsic transverse momentum k_T , 8 PDFs are needed:



Transverse Momentum Dependent PDFs

The three TMD PDFs below describe important properties of spin dynamics of nucleon.

$$f_{1T}^\perp(x, k_T^2)$$

: the Sivers effect describes the correlation of intrinsic transverse momentum of unpolarized quarks with nucleon transverse polarization.

$$h_1^\perp(x, k_T^2)$$

: the Boer-Mulders function describes the correlation between the transverse spin and the transverse momentum of a quark inside the unpolarised hadron.

$$h_{1T}^\perp(x, k_T^2)$$

: the Pretzelosity function describes the polarisation of a quark along its intrinsic k_T direction making accessible the orbital angular momentum information.

Single-polarised DY cross-section: Leading order QCD parton model

At LO the general expression of the DY cross-section simplifies to

(COMPASS Note 2010-2) :

$$\frac{d\sigma^{LO}}{d^4q d\Omega} = \frac{\alpha_{em}^2}{Fq^2} \hat{\sigma}_U^{LO} \left\{ \left(1 + D_{[\sin^2 \theta]}^{LO} A_U^{\cos 2\varphi} \cos 2\varphi \right) + |\vec{S}_T| \left[A_T^{\sin \varphi_s} \sin \varphi_s + D_{[\sin^2 \theta]}^{LO} \left(A_T^{\sin(2\varphi + \varphi_s)} \sin(2\varphi + \varphi_s) + A_T^{\sin(2\varphi - \varphi_s)} \sin(2\varphi - \varphi_s) \right) \right] \right\}$$

Thus the measurement of 4 asymmetries (modulations in the DY cross-section):

$$A_U^{\cos 2\varphi}$$

- gives access to the Boer-Mulders functions of the incoming hadrons,

$$A_T^{\sin \varphi_s}$$

- to the Sivers function of the target nucleon,

$$A_T^{\sin(2\varphi + \varphi_s)}$$

- to the Boer-Mulders functions of the beam hadron and to h_{1T}^\perp , the pretzelosity function of the target nucleon,

$$A_T^{\sin(2\varphi - \varphi_s)}$$

- to the Boer-Mulders functions of the beam hadron and to h_1 , the transversity function of the target nucleon.